

EE

Internal Report
DESY M-94-11
Oktober 1994

Design and Performance of a Symmetric High Power Coupler for a 6 Meter S-Band Linear Collider Accelerating Structure

See 9503

by

V.E. Kaljuzhny, V.E. Kandrunin, D.V. Kostin,
S.V. Ivanov, O.S. Milovanov, N.N. Nachaev,
A.N. Parfenov, N.P. Sobenin, S.N. Yaragin

*Moscow Engineering Physics Institute, MEPI
Kashirskoe shosse, 31, 115409 Moscow, Russia*

L.V. Kravchuk, G.V. Romanow, A.N. Stepanov
A.V. Vaysuchenko, I.N. Zelezov

*Institute of Nuclear Research, INR
Profsojuznaja 7a, 117312 Moscow, Russia*

M. Dohlus, N. Holtkamp

*Deutsches Elektronen-Synchrotron, DESY
Notkestraße 85, 22607 Hamburg, Germany*



2 Contents

	2
2 CONTENTS	3
3 INTRODUCTION	4
4 COUPLER TUNING METHOD	5
5 COUPLER PARAMETER MEASUREMENTS	10
6 COUPLER TUNING	12
7 IMPEDANCE CHARACTERISTICS	20
8 COUPLER FIELD ASYMMETRY	20
9 T-JUNCTION	30
10 REFERENCES	32

4 COUPLER TUNING METHOD

Let's consider the basic principles of the coupler tuning method with the use of the additional waveguides having the shorting plungers. The method is the same for both the input and output couplers of a 6 m. length accelerating section with changing dimensions and $\frac{2\pi}{3}$ - mode at 2998 MHz [3].

In fig.1 the reference planes for T-junction and 4-port device made of a coupler and connecting waveguides are shown by dotted lines. The reference planes of the T-junction are chosen in such a way that the scattering matrix of the T-junction has the following form :

$$|S|_T = \begin{vmatrix} 0 & \frac{1}{\sqrt{2}} & \frac{1}{\sqrt{2}} \\ \frac{1}{\sqrt{2}} & \frac{1}{2} & -\frac{1}{2} \\ \frac{1}{\sqrt{2}} & -\frac{1}{2} & \frac{1}{2} \end{vmatrix} \quad (1)$$

The reference planes of the 4-port device are situated in symmetrical way with respect to the coupler feeding slots. Their positions are chosen so that when the coupler is replaced by a single resonator with the resonant frequency f_0 and the own Q -factor value Q_0 the scattering matrix of such a system would have the following form

$$|S| = \begin{vmatrix} S_{11} & S_{12} & S_{11} & S_{11} \\ S_{12} & S_{11} & S_{11} & S_{11} \\ S_{11} & S_{11} & S_{11} & S_{12} \\ S_{11} & S_{11} & S_{12} & S_{11} \end{vmatrix} \quad (2)$$

where

$$S_{11} = \frac{\chi}{1 + 2\chi + jQ_0 \left(\frac{f}{f_0} - \frac{f_0}{f} \right)}$$

$$S_{12} = -\frac{1 + \chi + jQ_0 \left(\frac{f}{f_0} - \frac{f_0}{f} \right)}{1 + 2\chi + jQ_0 \left(\frac{f}{f_0} - \frac{f_0}{f} \right)} \quad (3)$$

χ is the coefficient of cavity coupling with every waveguide. The positions of short-circuited plungers are characterized by

$$\psi = \pi - 4\pi \frac{\Delta l}{\lambda_w} \quad (4)$$

Δl is the distance between the reference plane and the short-circuited plunger, Δl is being negative if the plungers are displaced from the resonator and Δl is being positive if they are displaced to the resonator, λ_w is the wavelength in the waveguides.

If a single resonator is used the reflection coefficient at the input of the T-junction can be written as

$$\Gamma = \frac{2S_{11} - (4S_{11} - 1)e^{j\psi}}{1 - 2S_{11}e^{j\psi}} = \frac{2\chi - \left[2\chi - 1 - jQ_0 \left(\frac{f}{f_0} - \frac{f_0}{f}\right)\right] e^{j\psi}}{2\chi + 1 + jQ_0 \left(\frac{f}{f_0} - \frac{f_0}{f}\right) - 2\chi e^{j\psi}} \quad (5)$$

Let us now consider a coupler which is fed through rectangular waveguides and is connected with the infinite uniform disk-loaded circular lossless waveguide. To obtain the expression for the reflection coefficient we use the resonant model of the coupler and disk-loaded waveguide (DLW), which is introduced in [4]. According to this model the DLW is represented by a chain of identical cells (resonators) which are characterized by the resonance frequency f_r and coupling coefficient with adjacent cells $\frac{K_0}{2}$. The coupler is also represented by a resonator with the resonance frequency f_c , coupling coefficient with each of connecting waveguides χ and the own Q -factor Q_c . The coupling between the coupler and the first cell of the DLW is denoted $\frac{K_c}{2}$, generally K_c not being equal to K_0 . It should be noted that in the model under consideration the frequencies f_r and f_c are the frequencies where the cells and the coupler are excited under the condition that there are no fields in adjacent cells and the corresponding coupling elements are not perturbed.

The dispersion characteristic of the infinite uniform DLW without losses has the following form

$$f = f_r \sqrt{1 - K_0 \cos \varphi}, \quad (6)$$

where φ is the mode corresponding to the frequency f . It is assumed that at all DLW passband frequencies the travelling wave regime is realized and the DLW itself can be considered as a transmission line connected to the coupler. Then the coupling between the DLW and the coupler can be written as

$$\chi_{DLW}(f) = Q_c \frac{K_0}{2} \left(\frac{K_c}{K_0}\right)^2 \frac{f_c \sin \varphi}{f} \quad (7)$$

and is frequency dependent. The frequency f and the mode φ in (7) are interconnected by the dispersion relation (6).

To provide the travelling wave regime in the DLW having the operational mode φ_{0w} at the frequency f_{0w} it is necessary that the cell frequencies should have the following form

$$f_r = \frac{f_{0w}}{\sqrt{1 - K_0 \cos \varphi_{0w}}} \quad (8)$$

The reflection coefficient at the input of a T-junction connected with the coupler and infinite uniform lossless DLW is defined by

$$\Gamma = \frac{2\chi - \left[2\chi - 1 - \chi_{DLW}(f) - jQ_c \left(\frac{f}{f_c} - \frac{f_c}{f} + \frac{f_c K_0}{f} \left(\frac{K_c}{K_0} \right)^2 \cos \varphi \right) \right] e^{j\psi}}{2\chi + 1 + \chi_{DLW}(f) + jQ_c \left(\frac{f}{f_c} - \frac{f_c}{f} + \frac{f_c K_0}{f} \left(\frac{K_c}{K_0} \right)^2 \cos \varphi \right) - 2\chi e^{j\psi}} \quad (9)$$

It follows from (9) that the reflection coefficient equals zero at the operational frequency if :

$$f_c = \frac{f_{0w}}{\sqrt{1 - \frac{K_0}{2} \left(\frac{K_c}{K_0} \right)^2 \cos \varphi_{0w}}}$$

$$\psi = \pi; \Delta l = 0; \quad (10)$$

$$4\chi = 1 + \chi_{DLW}(f_{0w}) = 1 + Q_c \frac{K_0}{2} \left(\frac{K_c}{K_0} \right)^2 \frac{\sin \varphi_{0w}}{\sqrt{1 - \frac{K_0}{2} \left(\frac{K_c}{K_0} \right)^2 \cos \varphi_{0w}}}$$

Notice that at $\psi = 0$ or $\psi = 2\pi$ the reflection coefficient $\Gamma = 1$ is irrespective of f, f_0 or Q_c and χ_{DLW} .

Thus for the matching it is necessary to place the short-circuiting plungers strictly at the reference planes and realize the tuning of the coupler with respect to the frequency and coefficient of coupling with connecting waveguides. If the matching conditions (10) are met the reflection coefficient can be written as

$$\Gamma = \frac{\sin \varphi_{0w} - \frac{f_{0w}}{f} \sin \varphi - j \frac{1 - \frac{1}{2} \left(\frac{K_c}{K_0} \right)^2}{\frac{K_0}{2} \left(\frac{K_c}{K_0} \right)^2} \left(\frac{f}{f_{0w}} - \frac{f_{0w}}{f} \right)}{2 \frac{\sqrt{1 - \frac{K_0}{2} \left(\frac{K_c}{K_0} \right)^2 \cos \varphi_{0w}}}{Q_c \frac{K_0}{2} \left(\frac{K_c}{K_0} \right)^2} + \sin \varphi_{0w} + \frac{f_{0w}}{f} \sin \varphi + j \frac{1 - \frac{1}{2} \left(\frac{K_c}{K_0} \right)^2}{\frac{K_0}{2} \left(\frac{K_c}{K_0} \right)^2} \left(\frac{f}{f_{0w}} - \frac{f_{0w}}{f} \right)} \quad (11)$$

Because usually $Q_c \frac{K_0}{2} \left(\frac{K_c}{K_0} \right)^2 \gg 1$ and the operational mode φ_{0w} is $\frac{\pi}{2}$ or $\frac{2\pi}{3}$ the expression 11 can be written in the approximate form:

$$\Gamma = \frac{\sin \varphi_{0w} - \frac{f_{0w}}{f} \sin \varphi - j \frac{2}{K_0} \left[\left(\frac{K_0}{K_c} \right)^2 - \frac{1}{2} \right] \left(\frac{f}{f_{0w}} - \frac{f_{0w}}{f} \right)}{\sin \varphi_{0w} + \frac{f_{0w}}{f} \sin \varphi + j \frac{2}{K_0} \left[\left(\frac{K_0}{K_c} \right)^2 - \frac{1}{2} \right] \left(\frac{f}{f_{0w}} - \frac{f_{0w}}{f} \right)} \quad (12)$$

As earlier shown the frequency f and the mode φ are correlated by dispersion equation (6).

If an additional condition

$$\left(\frac{K_c}{K_0}\right)^2 = 2 \quad (13)$$

can be met then

$$f_c = f_r = \frac{f_{0w}}{\sqrt{1 - K_0 \cos \varphi_{0w}}} \quad (14)$$

and the expressions (12) become

$$\Gamma = \frac{f \sin \varphi_{0w} - f_{0w} \sin \varphi}{f \sin \varphi_{0w} + f_{0w} \sin \varphi} \quad (15)$$

It can be seen from (15) that at accomplishing of conditions (13) and (10) the reflection coefficient is really over all DLW passband and the coupler appears to be optimal as far as the broad band matching is concerned. But in practice the condition (13) is not met and usually the values of K_c and K_0 differ slightly. In particular if the length of the coupler and all the cells are the same and all disks including the first are identical nevertheless $K_c \neq K_0$ due to the coupling slots and the beam hole, K_c is less than K_0 .

Thus for the coupler tuning it is necessary to have a possibility to determine experimentally positions of the short-circuiting plungers at $\psi = \pi$ as well as the coupler parameters: f_c , $\frac{K_c}{2}$ or $\frac{K_c}{K_0}$, 4χ or $\frac{Q_c}{4\chi}$. The DLW cell parameters are assumed to be known (f_{0w} , f_r , K_0 , φ_{0w}). When the first DLW cell (adjacent to the coupler) is strongly detuned expression (9) can be rewritten as

$$\Gamma_1 = \frac{2\chi - \left[2\chi - jQ_c \left(\frac{f}{f_c} - \frac{f_c}{f}\right)\right] e^{j\psi}}{2\chi + jQ_c \left(\frac{f}{f_c} - \frac{f_c}{f}\right) - 2\chi e^{j\psi}} \quad (16)$$

taking into account that $2\chi \gg 1$.

When the coupler is strongly detuned we have

$$\Gamma_0 = e^{j\psi} \quad (17)$$

Expression (17) is valid irrespectively of the frequency f if it is inside the DLW passband. From (16) and (17) we have

$$\begin{aligned} \Gamma_1(f = f_c) &= +1 = e^{j0} \\ \Gamma_0(f = f_c) &= e^{j\psi} \end{aligned} \quad (18)$$

Moreover, if $\psi = \pi$ then $\Gamma_1(f = f_c \pm \Delta f) = e^{\pm j\alpha}$, where $\alpha = -2\text{arctg} \left[\frac{Q_c \Delta f}{2\chi f_c} \right]$ at $\Delta f \ll f_c$.

So by means of measurement the reflection coefficients Γ_1 and Γ_0 arguments can be experimentally determined the coupler resonant frequency as well as the ratio $\left(\frac{Q_c}{4\chi}\right)$. For this purpose at some position short-circuited plungers we find the frequency f_1 at which $\arg\Gamma_1(f_1) - \arg\Gamma_0(f_1) = \pm\pi$. Then if $\arg\Gamma_1(f_1 - \Delta f) + \arg\Gamma_1(f_1 + \Delta f) = 2\arg\Gamma_1(f_1)$, we have $\psi = \pi$ and $f_1 = f_c$. In case this condition for Γ_1 arguments is not met we have to replace the positions of the short-circuiting plungers and repeat the measurements with new positions. It should be noticed that if $\arg\Gamma_1(f_1 - \Delta f) + \arg\Gamma_1(f_1 + \Delta f) > 2\arg\Gamma_1(f_1)$ the plunger had to be replaced towards the coupler and vice versa.

The experimental determination of the coefficient of coupling between the coupler and the first DLW cell is based on the fact that with strong detuning of the second cell and equality of the coupler and first cell frequencies there are two frequencies f_1 and f_2 when

$$\begin{cases} \arg\Gamma_2(f_1) - \arg\Gamma_0(f_1) = \pm\pi \\ \arg\Gamma_2(f_2) - \arg\Gamma_0(f_2) = \pm\pi \end{cases} \quad (19)$$

where Γ_2 is the reflection coefficient when the second cell is strongly detuned.

Notice that if the first cell frequency is equal to f_c we have $\arg\Gamma_2(f_c) = \arg\Gamma_0(f_c)$.

The coupling coefficient can be determined in terms of experimentally obtained frequencies f_1 and f_2 at which the conditions (19) are met and the first cell frequency is equal to f_c

$$\frac{K_c}{2} = \frac{|f_1^2 - f_2^2|}{f_1^2 + f_2^2} \quad (20)$$

In particular, when $\varphi_{0w} = \frac{2\pi}{3}$ and $f_{0w} = f_{\frac{2\pi}{3}}$ and also the matching requirements 10 are met, i.e.

$$\begin{aligned} \psi = \pi, \quad f_c &= f_{\frac{2\pi}{3}} \left[1 + \frac{K_0}{4} \left(\frac{K_c}{K_0} \right)^2 \right]^{-\frac{1}{2}} \\ \frac{Q_c}{4\chi} &= \frac{2}{K_0} \left(\frac{K_0}{K_c} \right)^2 \frac{2}{\sqrt{3}} \sqrt{1 + \frac{K_0}{4} \left(\frac{K_c}{K_0} \right)^2} \end{aligned} \quad (21)$$

then at $f = f_{\frac{2\pi}{3}}$ we have

$$\arg\Gamma_1 \left(f_{\frac{2\pi}{3}} \right) = -2\arctg \left[\frac{Q_c}{4\chi} \left(\frac{f_{\frac{2\pi}{3}}}{f_c} - \frac{f_c}{f_{\frac{2\pi}{3}}} \right) \right] = -2\arctg \left(\frac{1}{\sqrt{3}} \right) = -60^\circ \quad (22)$$

So in this particular case when conditions (21) are met we have

$$\begin{aligned} \arg\Gamma_0(f_c) &= \arg\Gamma_0(f_{\frac{2\pi}{3}}) = \pm\pi \\ \arg\Gamma_1(f_c) &= 0 \end{aligned}$$

$$\arg\Gamma_1(f\frac{2\pi}{\lambda}) = -60^\circ$$

These relations can be used for checking the accuracy of coupler tuning.

5 COUPLER PARAMETER MEASUREMENTS

Now consider experiments for the determination of the coupler parameters: f_c , $\frac{Q_c}{4\lambda}$, $\frac{K_c}{2}$. In fig.2 a prototype scheme for the measurement of the coupler frequency and the ratio $\frac{Q_c}{4\lambda}$ is presented.

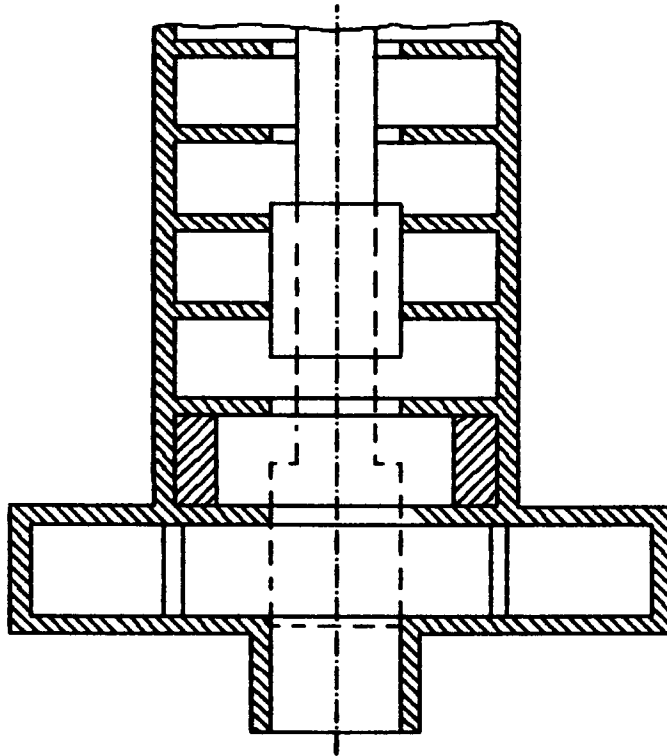


Fig.2 : Schematic drawing of experimental model for measurement of the coupler parameters (f_c , $\frac{Q_c}{4\lambda}$).

The coupler detuning is reached by means of a movable plunger which can be inserted inside the coupler over its full height and diameter which is equal to that of disk holes (the plunger position at the moment of detuning is shown by dashed lines in fig.2). The detuning of the first cell is realized by means of a thick ring , the plunger being positioned as shown by solid lines in fig.2. The required detuning

of the first cell should be more than 1500 MHz. The operational first cell frequency which normally is about 3000 MHz should be increased in the process of detuning. This process has to be realized in such a way that there is no field perturbation at the disk hole between the coupler and the first cell.

The prototype scheme for the experimental determination of the coupling between the coupler and the first cell ($\frac{K_c}{2}$) is shown in fig.3. For the first cell frequency changing

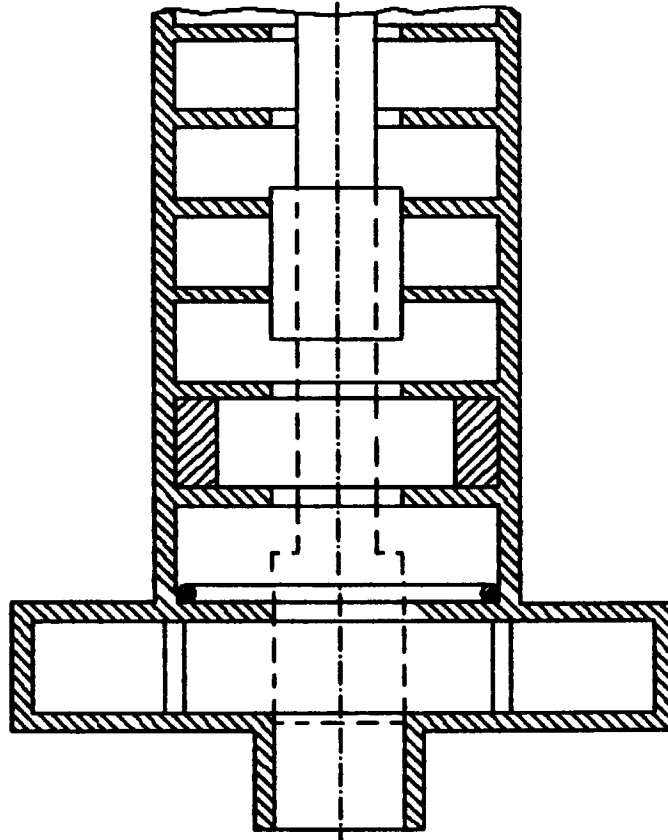


Fig.3 : Schematic drawing of experimental model for measurement of the coupling between the coupler and the first cell ($\frac{K_c}{2}$)

some tuning elements inside should be provided. By means of them one can realize the equality of the coupler and cell frequencies. The detuning of the second cell can also be realized by a thick ring while the coupler is detuned by the movable plunger (its position is shown by the dotted lines). When the plunger is placed in a position shown by solid lines in fig.3 its butt-end should be placed at the medium plane of the third cell (similar to the previous case of fig.2 when its butt-end is positioned at the

medium plane of the second cell).

In both cases the measurement of $\arg\Gamma_0$ is carried out with the plunger positioned inside the coupler, but the measurement of $\arg\Gamma_1$ and $\arg\Gamma_2$ with the plunger positioned in cells. Each time the determination of $\arg\Gamma_1$ and $\arg\Gamma_2$ is realized at the frequency at which the measurement of $\arg\Gamma_0$ was realized.

So in every pair of measurement we can assume $\arg\Gamma_0 = 0$ and by this avoid the influence of the finite length of the waveguide net work on measurement results.

Experimentally determined and calculated parameters of the input and output cells are presented in Table.1, the experimentally determined parameters being related to matched couplers, where f_{r_1} is the resonance frequency of the cell adjacent to the coupler.

Table 1:

		k_c	f_c , MHz	$\frac{Q_{CL}}{4x}$	k_0	f_{r_1} , MHz	$ \Gamma $
Input coupler	calculated	–	2991,19	51,3	0,04525	2963.2	0,0
	experimental	0,0455	2983.0	52,5	–	2962.1	0,065
Output coupler	calculated	–	2992,68	170,4	0,01423	2987,4	0,0
	experimental	0,0139	2991.7	173,5	–	2986.5	0,020

6 COUPLER TUNING

The development and experimental study of the coupler for DESY accelerating section were carried out separately for the input and output ends of the section. For this purpose DLW sections consisting of 11 cells with dimensions $a/\lambda = 0.1551$ and $a/\lambda = 0.10885$ (a this is the disk hole diameter), the structure period is 33.33 mm and cell shape is as in [3]. Keeping in mind that the sections would be operated in a condition vacuum and at the temperature of 40° C for the purpose of fine tuning of DLW cells to the frequency of 2998 MHz the changing of cell outer diameter was provisioned by means of wall deformations in four points. For this purpose 4 holes with a diameter of 12 mm were drilled in each cell so that the wall thickness was 1mm. The tuning was realized according to the technique described in [5] which takes into account the temperature, pressure and humidity at the moment of measurements. Thus, if this environmental parameters are $t = 18^\circ$ C, $p = 1000$ mB and humidity 50% then for obtaining the operational frequency 2998 MHz the cells should be tuned to the frequency 2998.16 MHz [5].

The connecting feeding guides ($72 \times 28, 33 \times 4$ mm) were fabricated out of standard rectangular waveguides with dimensions of $72 \times 34 \times 4$ mm, but the r.f. power divider was made from one piece of blank copper. For matching of the power divider a wedge

placed at the symmetry plane and an inductive slot were used.

All preliminary investigation connected with the coupler's optimal dimensions, determination as well as the measurement of its electrodynamic characteristics, were carried out on prototypes which consisted of a waveguide divider with transitions from $72 \times 28,33$ mm to 72×34 mm in cross-section, connecting rectangular waveguides with apertures (to make the subsequent coupler adjustment easier) as well as the coupler body, plungers and DLW cells. Also they include the device for fastening and moving the absorbing load and perturbing probes. The coupler fabrication tolerances on its inner dimensions as well as the short-circuiting plungers positions and those of T-junction matching elements were determined with these prototype schemes.

For the coupler prototype we made provisions for the construction elements soldering, replacement of choke plungers for short-circuited planes with adjustment screws as well as grooves for the coupler inner diameter adjustment.

The coupler dimensions such as the inner diameter $2b_c$ and coupling slot width $2a_c$ were first calculated on the basis of approximate resonator-analogue technique [6]. The tuning to the operational frequency was carried out by means of the technique described above and using of absorbing load [5].

The movable absorbing load technique enables us to determine the position of iconocenter (scattering matrix element S_{11}) by means of proper choice of the shape and surface resistance of the absorbing load. This technique is mostly suitable for VSWR values less than $1,5 \div 2$.

The best measurement results obtained for the input ends of the DLW with absorbing loads having the length about 3-4 cells length are presented in fig.4. The treatment of these results according to different techniques [5] resulted in the values of $|\Gamma|$ and φ with errors $\pm 5\%$, $\pm 2^\circ$.

By using absorbing loads it is possible to study the influence of $2b_c$ and $2a_c$ dimension variations on positions of the iconocenter in Smith's chart. As one example the corresponding results for the input and output couplers are shown in fig.5.

Since there would be no possibility of fine tuning by means of changing $2a_c$ in the working version of a coupler we have been considering a technique of fine tuning by changing the $2b_c$ and positions of short-circuited plungers. At the basis of such a technique the following arguments have been considered.

From (9) it follows that with changing of the short-circuiting plungers positions (that is the ψ value) the reflection coefficient Γ is changed in such a way (χ , Q_0 , f_c , $\chi_{DLW}(f_0)$, are all fixed) that in Smith chart the end of the complex vector Γ

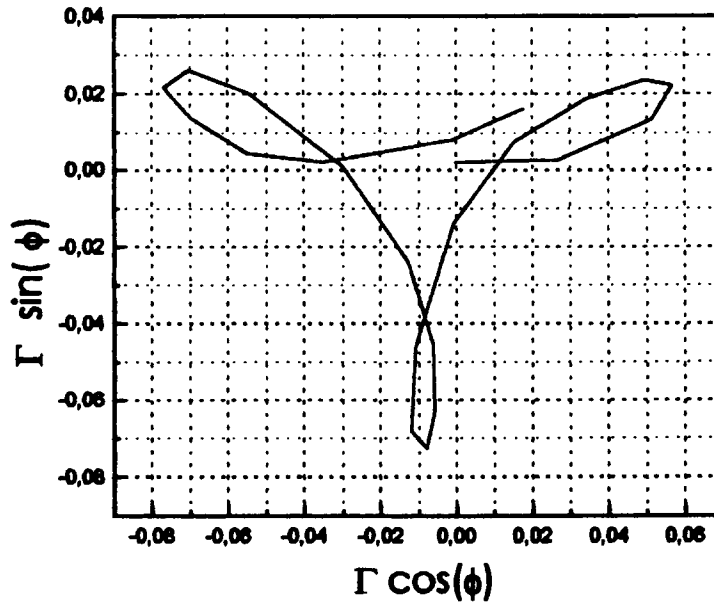


Fig.4 : The reflection coefficient depends on the position of the movable absorbing load in the input DLW.

would move along the circle passing through the point $\Gamma = 1$. When the frequency f_c changes the vector Γ end is also moving along the circle but the latter passes through the point $\Gamma = e^{j\psi}$. So the change of frequency and plunger positions leads to the replacement of the vector Γ end along crossing circles. Such circles are shown in fig.6 for the case when the coupling coefficient exceeds the required one (slightly overcoupled case) and the frequency f_c is less than the operational one. The initial plunger position was corresponded to $\psi_0 = \pi$. When $\psi_0 \neq \pi$ we have the case marked by dotted lines in the same figure. Thus we can make a conclusion that if the circle $\Gamma(f_c)$ surrounds the Smith chart center then in some cases it's possible to improve the matching by means of plungers removing (the initial points 1 and 1' as well as point 2). For obtaining the matching the frequency f_c should be changed so that the initial point (1 or 1') would be placed on the circle $\Gamma(\psi)$ passing through the Smith chart center.

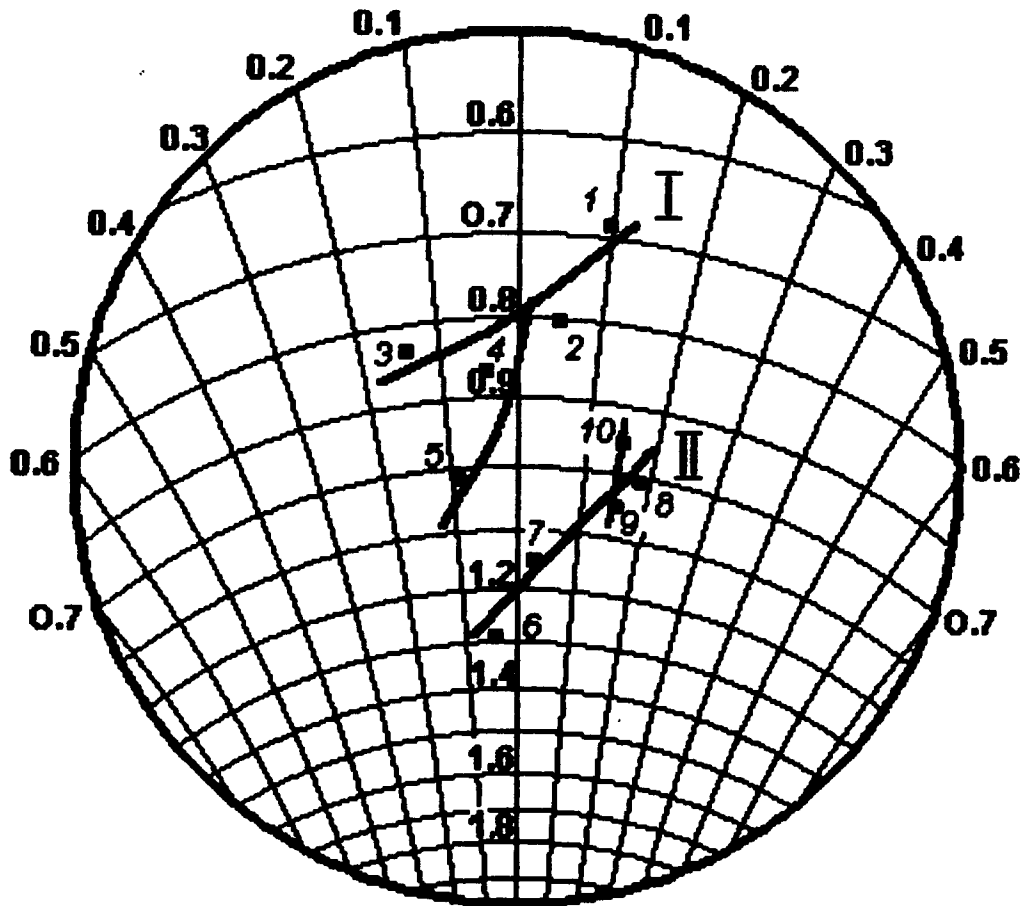


Fig.5 :Impedance variations at input (I) and output (II) couplers with changing dimensions $2b_c$ and $2a_c$.

1. $2b_c = 75.90 \text{ mm}$, $2a_c = 36.1 \text{ mm}$; 2. $2b_c = 75.98 \text{ mm}$, $2a_c = 36.1 \text{ mm}$;
3. $2b_c = 76.03 \text{ mm}$, $2a_c = 36.1 \text{ mm}$; 4. $2a_c = 36.1 \text{ mm}$, $2b_c = 75.48 \text{ mm}$;
5. $2a_c = 36.19 \text{ mm}$, $2b_c = 75.48 \text{ mm}$; 6. $2b_c = 77.15 \text{ mm}$, $2a_c = 25.45 \text{ mm}$;
7. $2b_c = 77.25 \text{ mm}$, $2a_c = 25.45 \text{ mm}$; 8. $2b_c = 77.30 \text{ mm}$, $2a_c = 25.45 \text{ mm}$;
9. $2a_c = 25.45 \text{ mm}$, $2b_c = 77.30 \text{ mm}$; 10. $2a_c = 25.55 \text{ mm}$, $2b_c = 77.30 \text{ mm}$

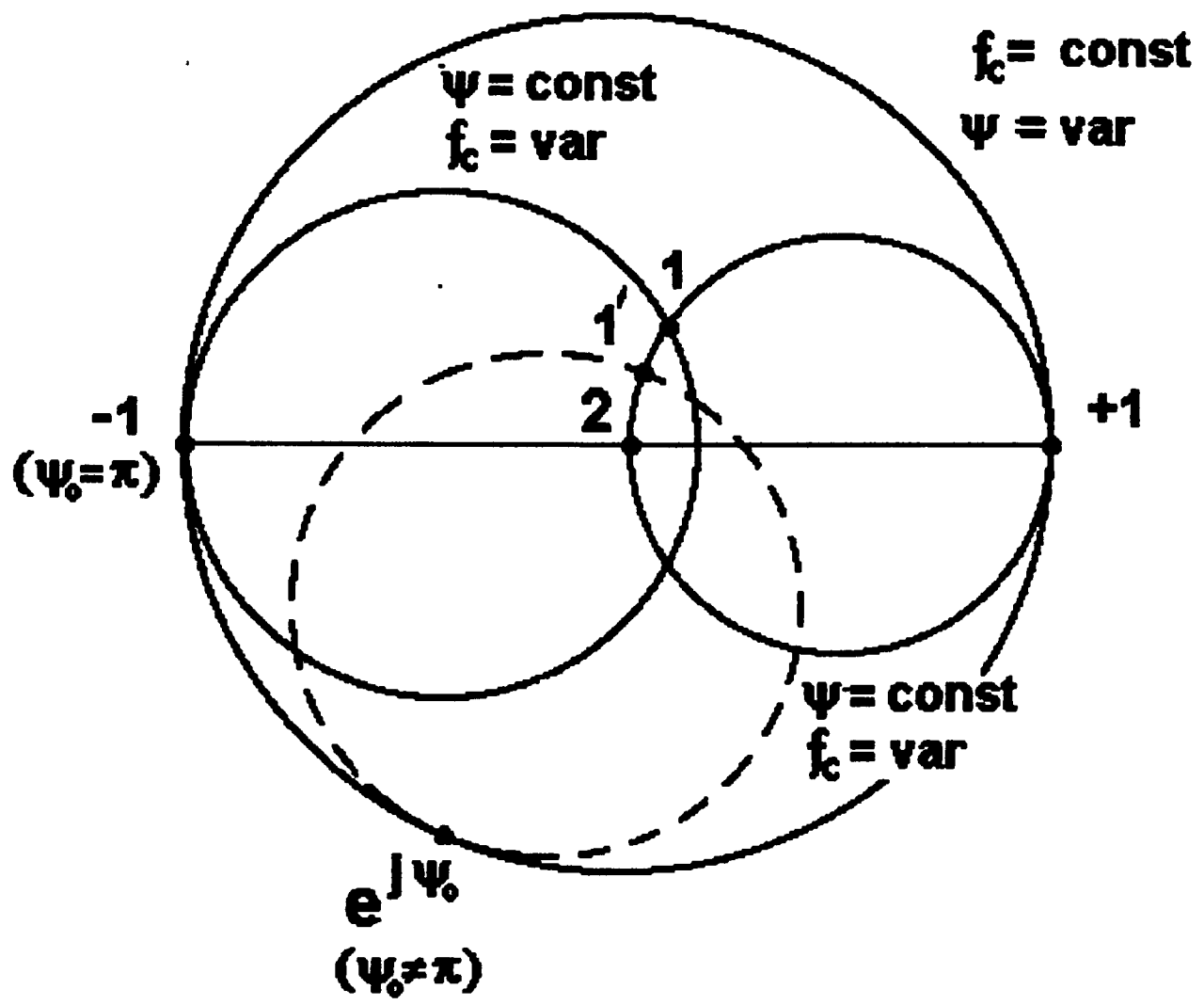


Fig.6 : Schematic of overloaded coupler tuning

It is very important to evaluate the fabrication tolerances (for dimensions $2b_c$ and $2a_c$) and that one position, of short-circuiting planes in the rectangular waveguides. The effect of $2b_c$ and $2a_c$ dimensions variations is shown in Fig.5. The tolerance on $2a_c$ dimension was fixed as ± 0.05 mm. The coupler inner diameter $2b_c$ tolerance should be ± 0.02 mm. Because the change of the coupler inner dimensions is not possible by the construction adjustment elements we have made provisions for $2b_c$ dimension variation by means of coupler wall deformations in four points. The results of the input coupler tuning at the by means of wall deformation in four points are presented in fig.7, the short-circuiting plunger position being displaced by ± 2 mm with respect to the nominal value.

By means of deformation the coupler butt wall insideward can be decreased the coupler own frequency and the requirements for coupler inner dimensions tolerances can be made less rigid and the tuning procedure can be made easier. For example the prototype input coupler own frequency was diminished by 8.7 MHz from 2982.7 MHz down to 2974 MHz that led to the VSWR change from 1.02 up to 1.41. It should be noted that the theoretical calculations according to the formula (11) obtained on the basis of the coupler equivalent circuit predicted almost the same frequency change 8.7 MHz with corresponding VSWR change from 1.00 up to 1.40. Due to the existence of such a possibility together with using four tuning elements to deform the coupler wall at the point where there is the magnetic field concentration the tolerances on the coupler inner diameter can be diminished to ± 0.04 mm. There is no "capacitive" tuning of the coupler own frequency for its working version due to inevitable constructional complications and necessity of one extra welding. So in the accepted coupler version instead of "capacitive" tuning we have used short-circuited plane position variation tuning.

The input coupler dimensions appeared to be $2b_c = 75.99 \pm 0.01$ mm, $2a_c = 36.5 \pm 0.05$ mm. The position of the short-circuits with respect to the middle gap was $\Delta Z_c = 26 \pm 0.1$ mm ($\Delta Z_c = 24 \pm 0.1$ mm for the prototype). The corresponding results for the output coupler were: $2b_c = 77.25 \pm 0.01$ mm, $2a_c = 25.55 \pm 0.05$ mm and $\Delta Z = 28 \pm 0.1$ mm ($\Delta Z_c = 24 \pm 0.1$ mm for the prototype).

To determine the influence of the coupler cell frequency f_c , the first cell frequency f_{r1} and the displacement of the short circuited planes with respect to their optimal position $\delta(\Delta Z_c)$ on matching of input and output couplers the calculations of the reflection coefficient values were carried out with variation of mentioned above parameters. The corresponding curves are shown in fig.8 and fig.9. Systems under consideration consisted of own frequencies and coupling coefficients equal to corre-

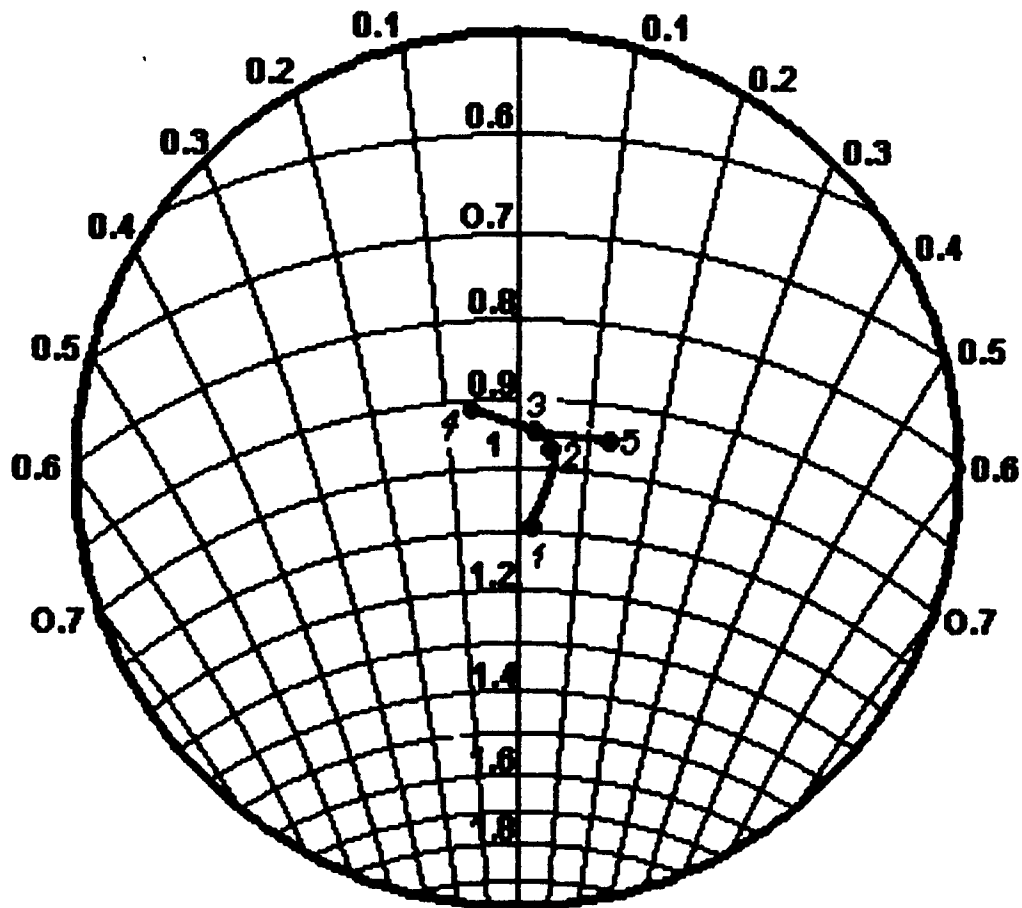


Fig.7 : Input coupler impedance variation dependson deformation of its side wall

- (1. $f_c = 2975.85$ MHz
- 2. $f_c = 2977.3$ MHz
- 3. $f_c = 2978.2$ MHz
- 4. $\Delta Z_c = 26$ mm
- 5. $\Delta Z_c = 22$ mm)

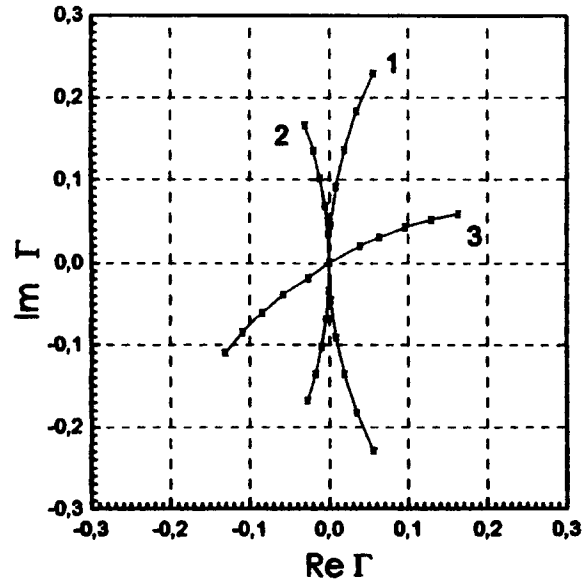


Fig.8 : Input coupler impedance characteristic dependson short-circuited plunger position (ΔZ), coupler resonance frequency (f_c), first cell frequency (f_{r1}).
 1 - $\delta\Delta Z = var (-10 \div +10 \text{ mm})$; 2 - $\delta f_c = var (-10 \div +10 \text{ MHz})$
 3 - $\delta f_1 = var (-10 \div +10 \text{ MHz})$

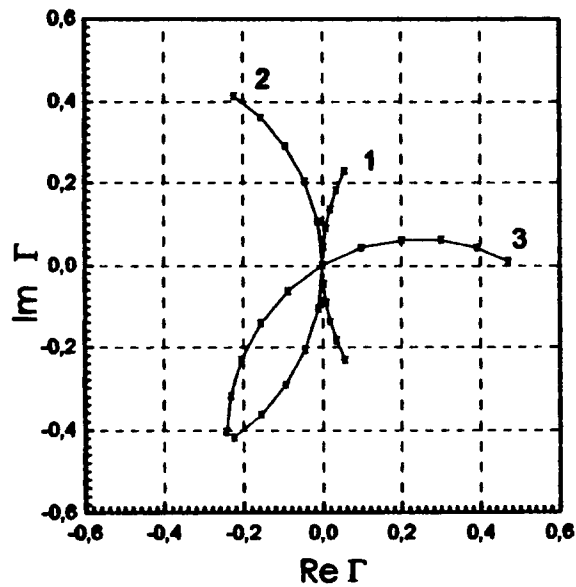


Fig.9 : Output coupler impedance characteristic dependson short-circuited plunger position (ΔZ), coupler resonance frequency (f_c), first cell frequency (f_{r1}).
 (Meaning of numbers is the same as in fig.8)

sponding values of the first and last cells of the acceleration section. The operational frequency was equal to $f_0 = 2998.00$ MHz. The last cell Q -factor was chosen of such a value that there was $2\pi/3$ - mode travelling wave regime at the frequency f_0 .

The calculation results are presented on Smith chart in the form of curves each of which corresponds to the variation of only one out of mentioned parameters, i.e. δf_c , δf_{r1} and $\delta(\Delta Z_c)$. Other parameters of couplers and DLW cells were assumed to have values corresponding to the ideal tuning and remained constant. ($\Delta Z_c = 24$ mm, $f_c = 2981.2$ MHz, $f_{r1} = 2963.2$ MHz for the input coupler and $\Delta Z_c = 26$ mm, $f_c = 2992.7$ MHz, $f_{r1} = 2987.4$ MHz for the output coupler).

7 IMPEDANCE CHARACTERISTICS

The calculated and experiment values of VSWR of the input working and output with 11 DLW cells are presented in fig.10 and fig.11. All cells had dimensions similar to the first cell or to the last cell.

The impedance characteristics of the 6 m length accelerating section with variable dimensions are shown in fig. 12 and fig.13.

8 COUPLER FIELD ASYMMETRY

Measurements of the field amplitude and phase asymmetry were realized according to the technique described in [1]. This technique of nonresonant perturbations is realized according to the scheme presented in [6]. The measurement accuracy greatly depends on the coupler tuning quality and obtaining the travelling wave regime in the DLW. The latter is obtained by means of a load having small reflection and an additional perturbing probe which compensates reflections in the DLW. With such a combination of the load and perturbing probe we succeeded in obtaining the reflection coefficient about 0.01.

The probe which is placed inside the coupler has cylindrical shape and is made of a dielectric with $\epsilon = 23$. Its length is 8 mm, the diameter 1 mm. It has the central hole with diameter 0.3 mm. If it is placed inside the waveguide with cross-section dimensions 72×34 mm and positioned at the medium plane with respect to the broad wall the reflection coefficient was 0.02 . Perturbing probes can be moved along Z coordinate with position uncertainty ± 0.01 mm. Also it can be moved along X and Y coordinates in the range ± 5 mm from the axis with corresponding error ± 0.1 mm.

In the process of the coupler field asymmetry measurements the reflection coefficient which is determined by means of a perturbation bead replacement along the

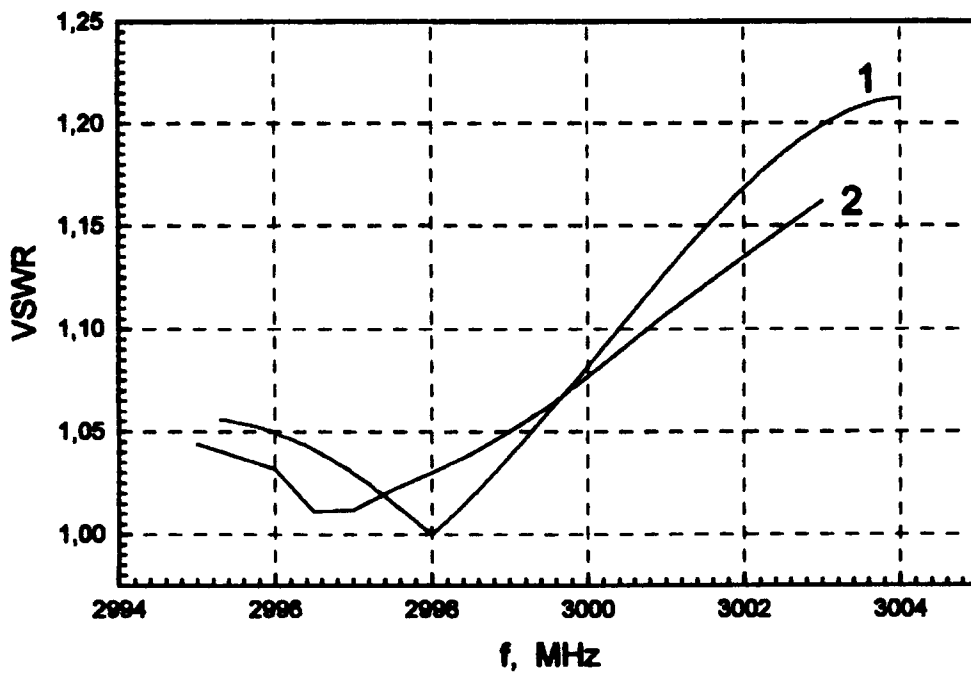


Fig.10 : The calculated (curve 1) and experimental (curve 2) values of VSWR for the input coupler with 11 DLW cells

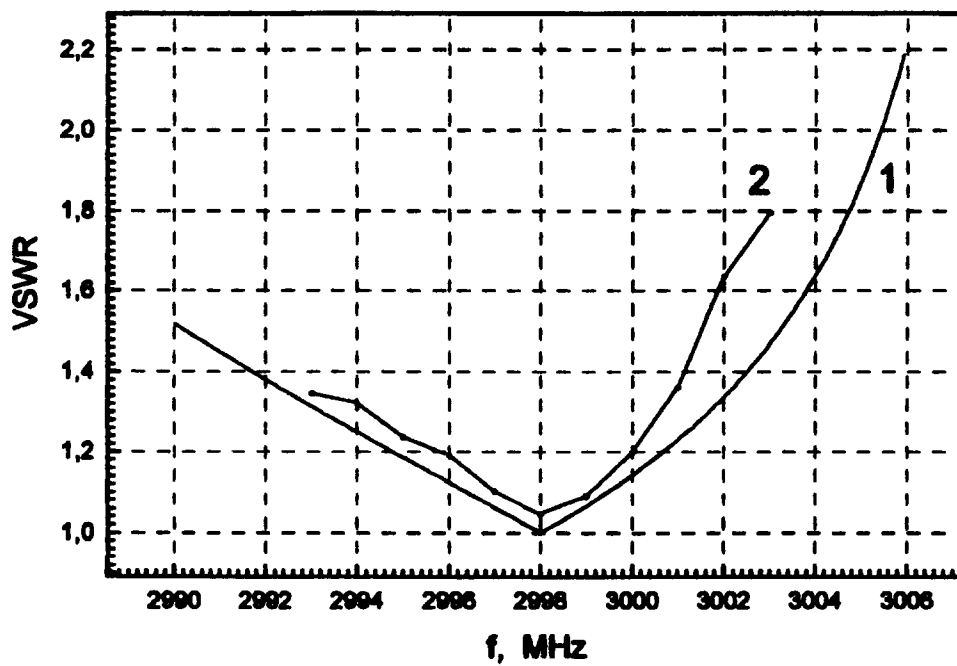


Fig.11 : The calculated (curve 1) and experimental (curve 2) values of VSWR for the output coupler with 11 DLW cells

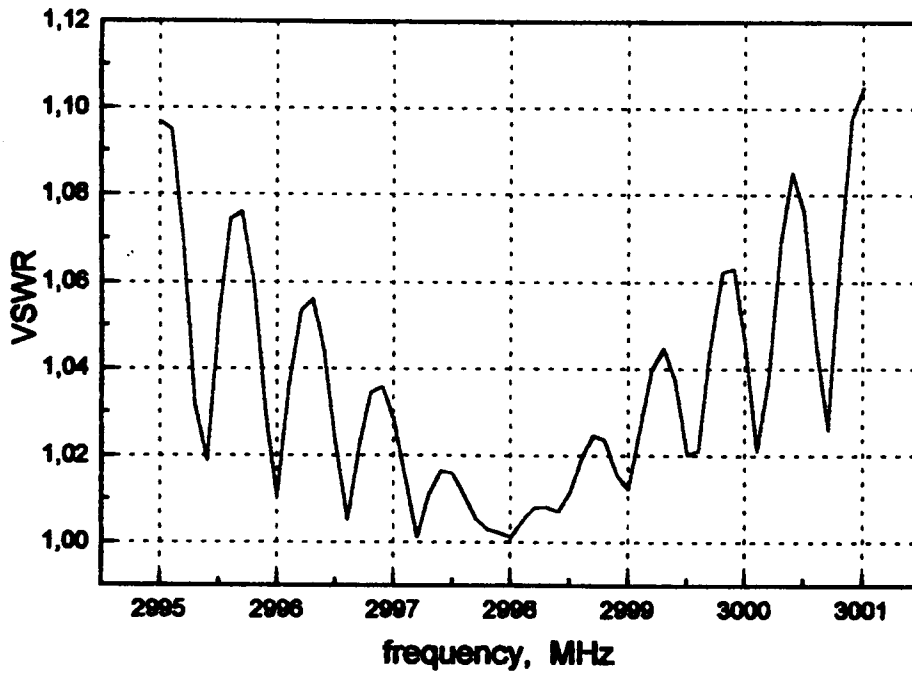


Fig.12 : The impedance characteristic of 6m length accelerating section with ideal tuned cells and matched couplers

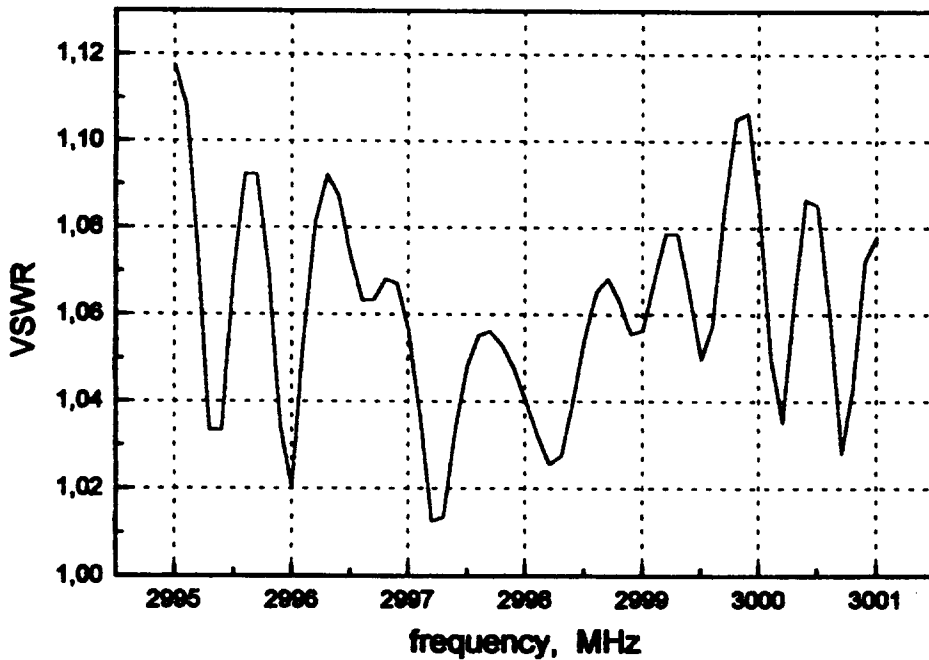


Fig.13 : The impedance characteristic of 6m length accelerating section when the cells frequencies and coupling coefficients have homogeneous dispersion

coordinate q should be generally presented as

$$\Gamma_{\Sigma}(q_i) = \Gamma_c + \Gamma_l + \Gamma_p(q_i) \quad (23)$$

where Γ_c is the reflection coefficient from the coupler, Γ_l is the reflection coefficient from the absorbing load, Γ_p is the reflection coefficient from a perturbation bead, which is to be determined.

The expression given above is valid only for small values of Γ_i ($\Gamma_i < 0.2$) and from it one can obtain

$$\Gamma_p(q_i) = \Gamma_{\Sigma}(q_i) - \Gamma_c - \Gamma_l$$

The values of Γ_c and Γ_l are determined with help of the loading curve obtained by means of measurements of the impedance at the coupler input with different positions of an absorbing load along the length of three DLW periods [5]. First load is set in the position where Γ_l is minimal. After determination of the iconocenter (point O at Smith's chart) the perturbing bead is inserted and again a new iconocenter position is determined (point O_2). The reflection coefficient from the perturbing bead $\Gamma_p(q_i)$ is now defined as the distance (vector) between points O and O_2 .

This technique could be simplified if the loading curve passes through the chart center, i.e. when we have $\Gamma_c + \Gamma_l = 0$. If the load is positioned in a way that this condition is met then after inserting a perturbing bead we can determine the reflection coefficient $\Gamma_p(q_i)$ from it as the vector between the Smith chart center and the newly found iconocenter.

Such measurements conducted for the output coupler have led to the following results :

$$\begin{aligned} \Gamma_p(q_i) &= 0.28e^{j180^\circ} && \text{(first technique) and} \\ \Gamma_p(q_i) &= 0.24e^{-j170^\circ} && \text{(second technique)} \end{aligned}$$

The values of $|\Gamma_c|$ and $|\Gamma_l|$ have not exceeded 0.2

In other schemes for obtaining the travelling wave regime in the DLW a matching section (transformer) is connected to the last cells by means of a coupling loop, the section having the absorbing load at its end. In the process of the transformer regulation the distributions of the electric field amplitude and phase along Z-direction were measured until the travelling wave regime was achieved. The corresponding distributions $\sqrt{\Gamma} = f(Z)$ and $\varphi = f(Z)$ are shown in fig.14 and 15 for the input coupler.

The measurements of $E \sim \sqrt{|\Gamma|}$ and φ as functions of X,Y coordinates were carried out for the inner input and output couplers

As an example the output coupler electric field longitudinal component which is proportional to the square root of the reflection coefficient from the perturbing

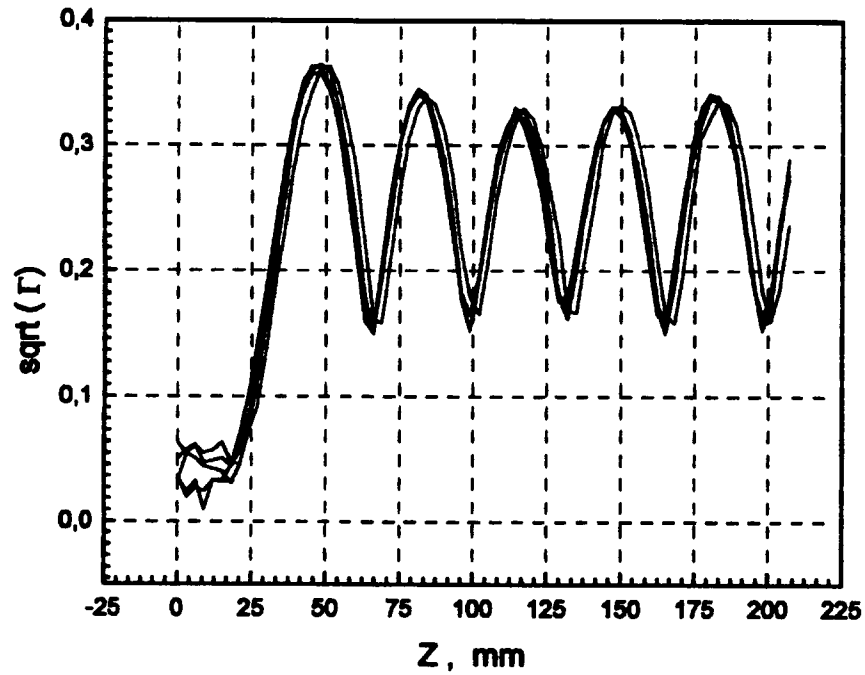


Fig.14 : Distribution of $\sqrt{\Gamma}$ depends on z-coordinate for the input coupler $x=0, y=0$; $x=-5 \text{ mm}, y=0$; $x=+5 \text{ mm}, y=0$; $x=0, y=-5 \text{ mm}$; $x=0, y=+5 \text{ mm}$

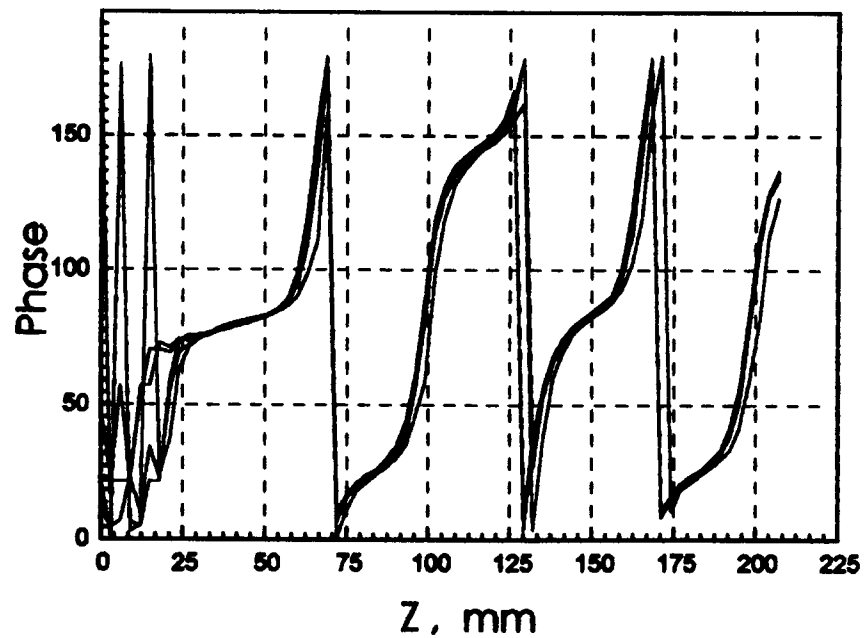


Fig.15 : Phase distribution depends on z-coordinate for the input coupler $x=0, y=0$; $x=-5 \text{ mm}, y=0$; $x=+5 \text{ mm}, y=0$; $x=0, y=-5 \text{ mm}$; $x=0, y=+5 \text{ mm}$

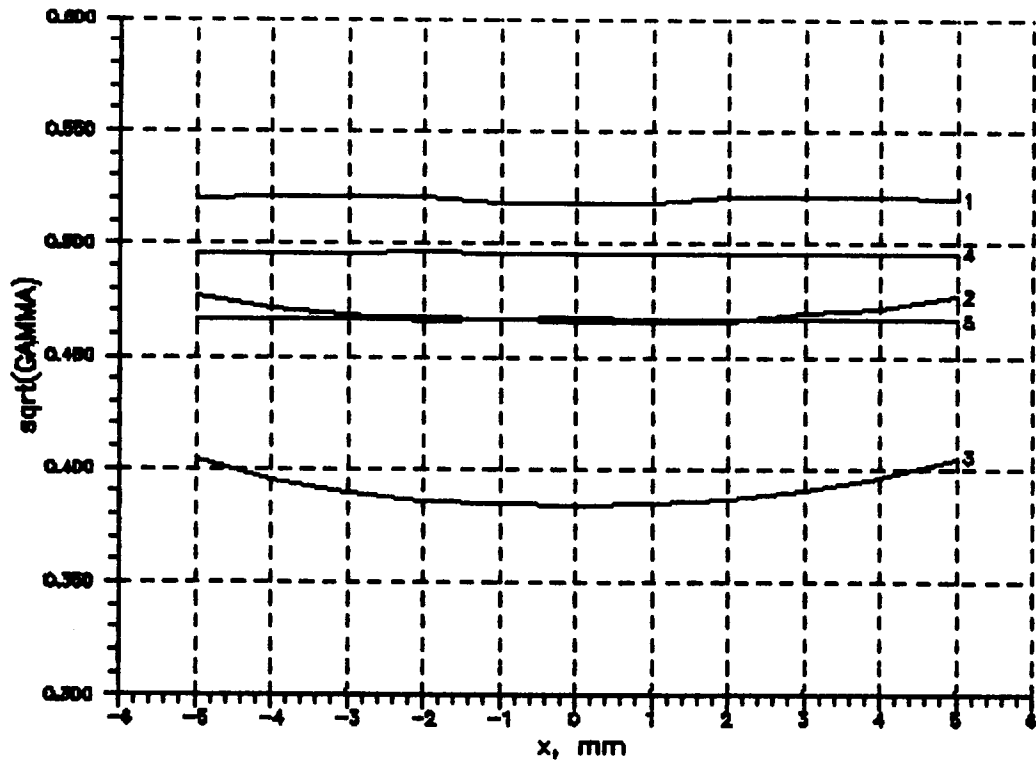


Fig.16a : Distribution of $\delta\Gamma$ depends on x-coordinate for the output coupler

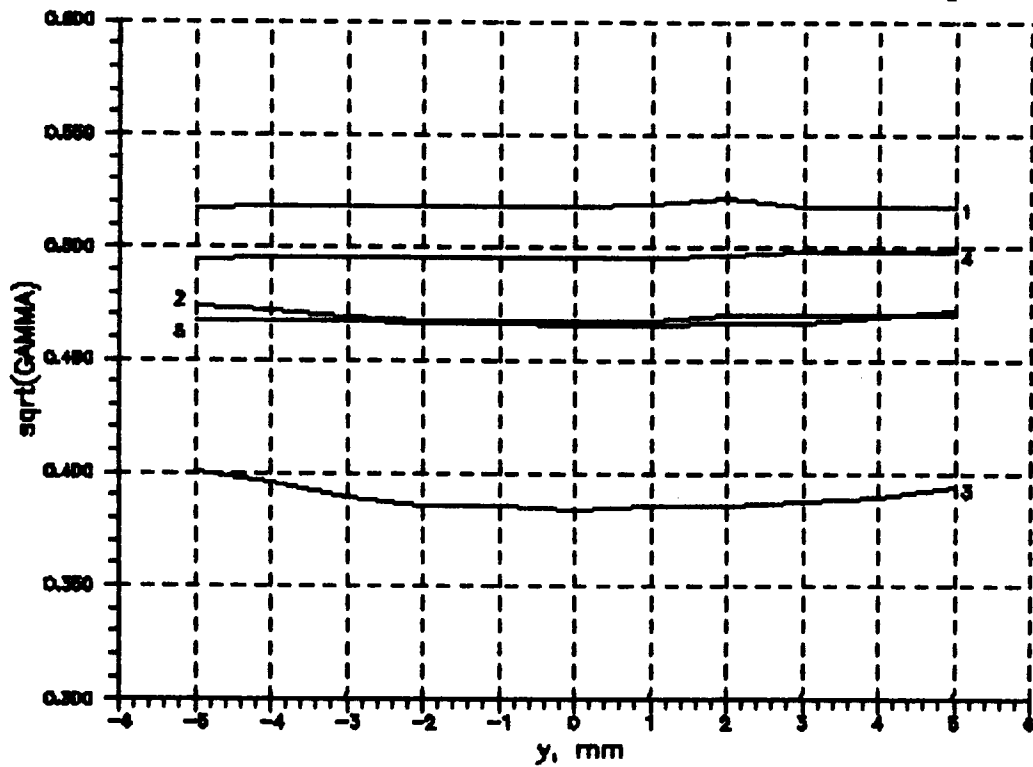


Fig.16b : Distribution of $\delta\Gamma$ depends on y-coordinate for the output coupler
 1 - Z=0 mm ; 2 - Z=5 mm ; 3 - Z=10 mm ; 4 - Z=-5 mm ; 5 - Z=-10 mm

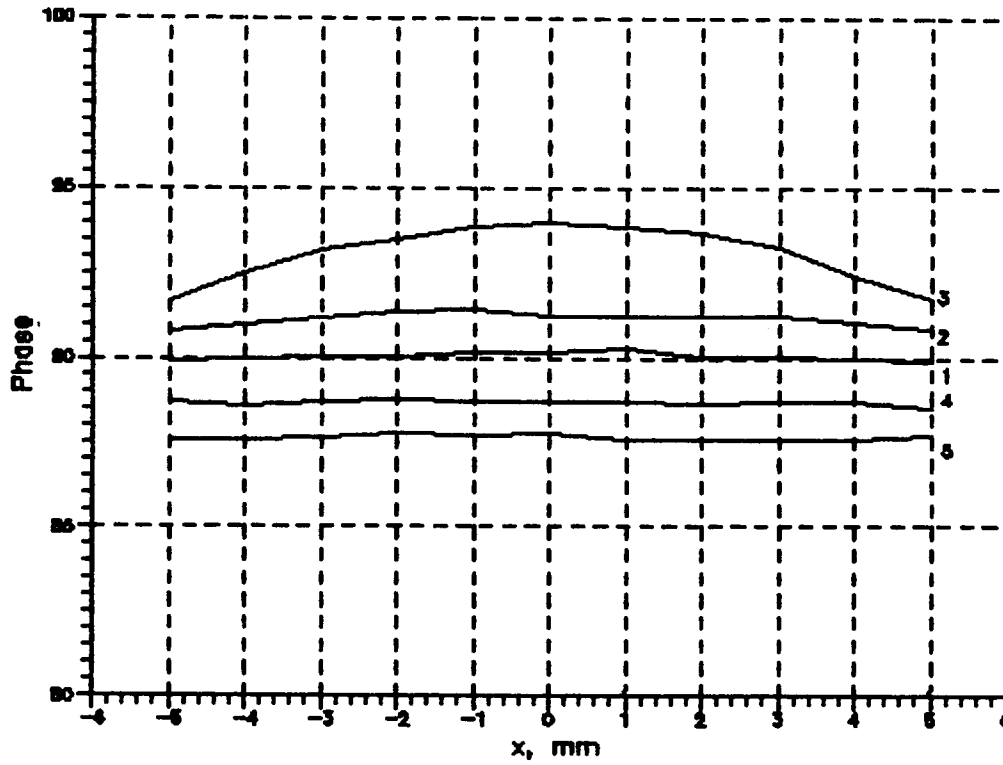


Fig.17a : Phase distribution depends on x-coordinate for the output coupler

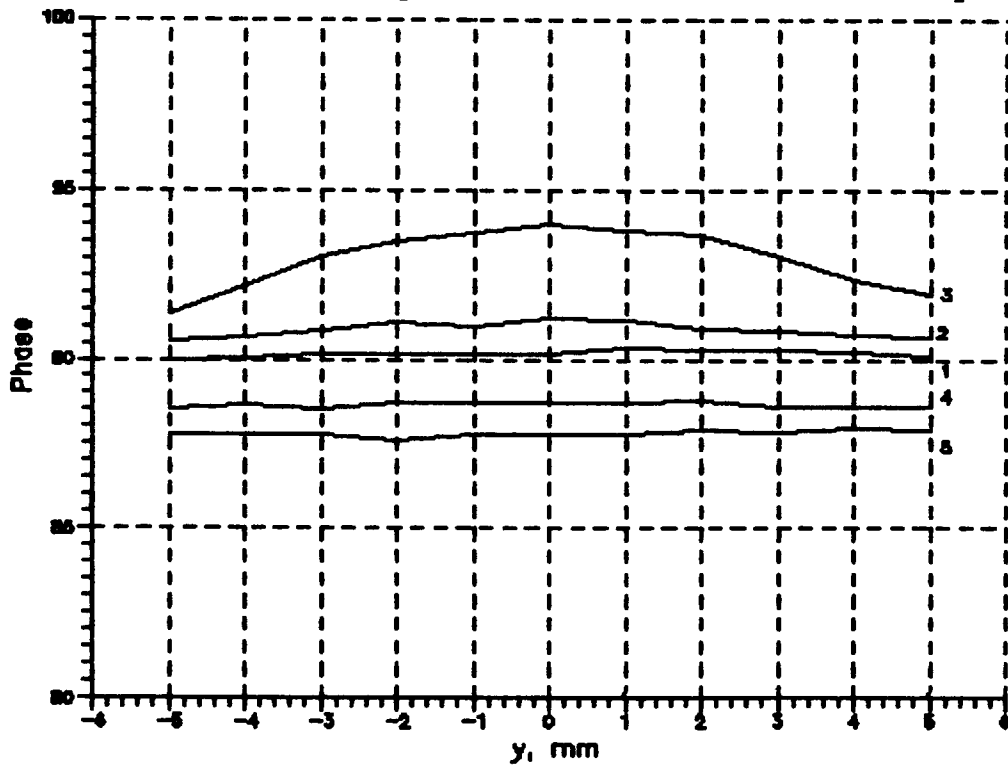


Fig.17b : Phase distribution depends on y-coordinate for the output coupler
 1 - Z=0 mm ; 2 - Z=5 mm ; 3 - Z=10 mm ; 4 - Z=-5 mm ; 5 - Z=-10 mm

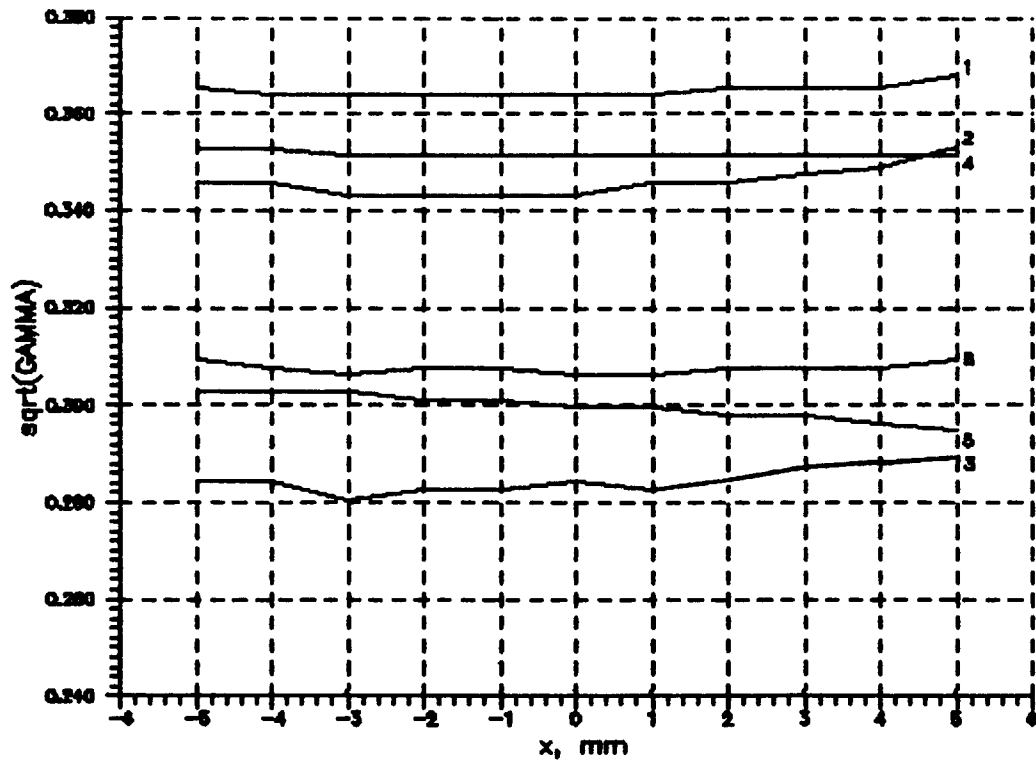


Fig.18a : Distribution of $\sqrt{\Gamma}$ depends on x-coordinate for the input coupler

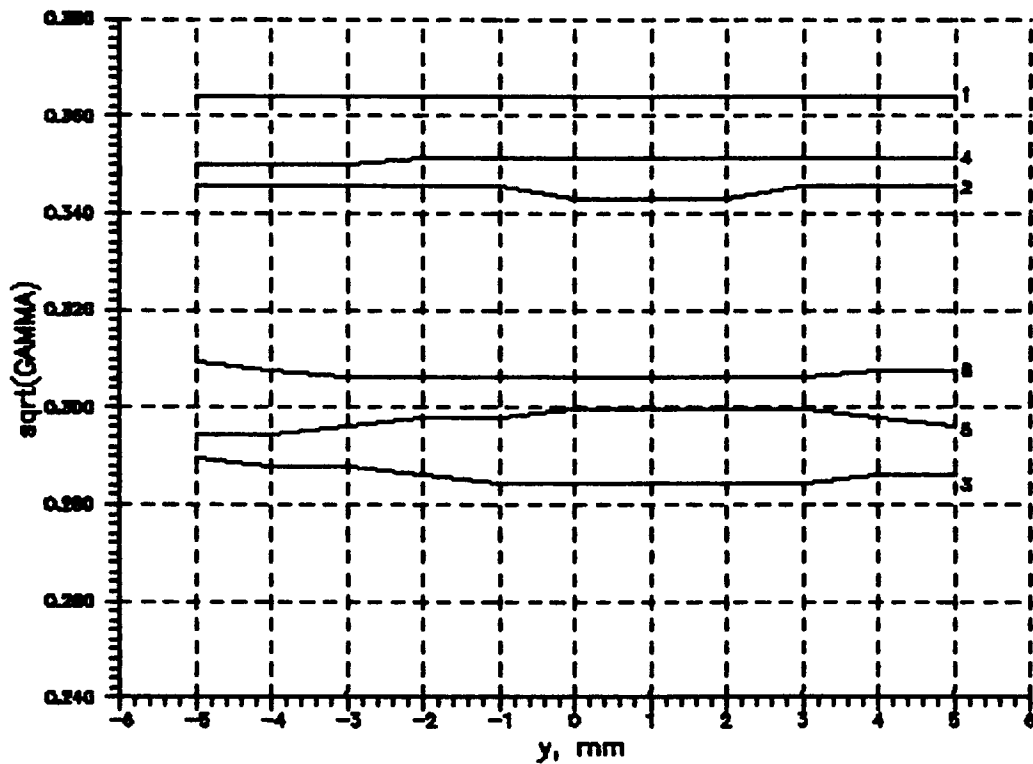


Fig.18b : Distribution of $\sqrt{\Gamma}$ depends on y-coordinate for the input coupler
 1 - Z=0 mm ; 2 - Z=5 mm ; 3 - Z=10 mm ; 4 - Z=-5 mm ; 5 - Z=-10 mm ;
 6 - Z=33 mm (center of the first cell)

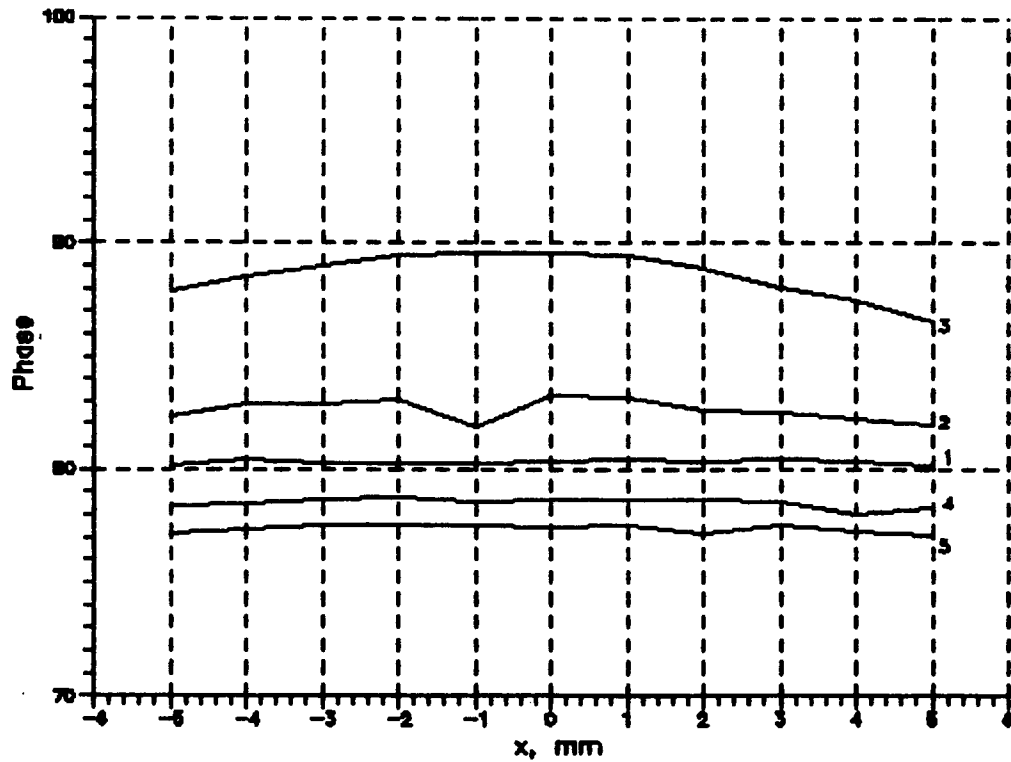


Fig.19a : Phase distribution depends on x-coordinate for the input coupler

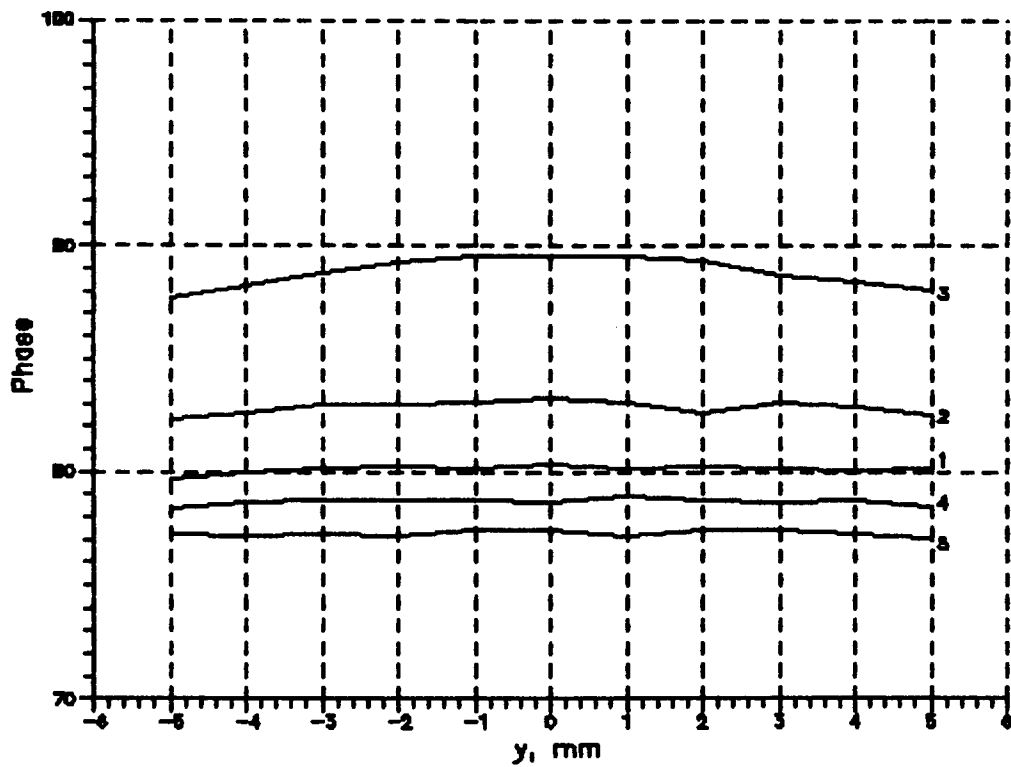


Fig.19b : Phase distribution depends on y-coordinate for the input coupler
 1 - $Z=0$ mm ; 2 - $Z=5$ mm ; 3 - $Z=10$ mm ; 4 - $Z=-5$ mm ; 5 - $Z=-10$ mm ;
 6 - $Z=33$ mm (center of the first cell)

bead versus X and Y coordinates is presented in fig.16a,b. There are 5 curves which correspond to different values of Z-coordinate . The value Z=0 correspond to the cavity medium plane . The phase distribution measurement results are shown in fig.17. This data analysis shows there is practically no field asymmetry with respect to X or Y coordinates.

For the quantitative evaluation of the field asymmetry along the cavity radius it's helpful to use normalized values:

$$\frac{h}{2r} = \frac{[E_z(x, 0) - E_z(0, y)]}{r [E_z(x, 0) + E_z(0, y)]}$$

$$\frac{\psi}{2r} = \frac{[\varphi(x, 0) - \varphi(0, y)]}{r [\varphi(x, 0) + \varphi(0, y)]}$$

where r is the radius value at which E_z and φ with respect to X and Y coordinates are determined.

Within r variation limit $r \leq 5$ mm maximal value of the parameters $\frac{h}{2r}$ and $\frac{\psi}{2r}$ appeared to be $0.0005 \frac{1}{\text{mm}}$ and $0.0002 \frac{\text{degree}}{\text{mm}}$ correspondingly. That guarantees good field symmetry inside the coupler cavity.

Similar data for the input coupler are presented in fig.18 and fig.19. The maximal values of $\frac{h}{2r}$ and $\frac{\psi}{2r}$ in this case are equal to $0.0013 \frac{1}{\text{mm}}$ and $0.0002 \frac{\text{degree}}{\text{mm}}$.

The slot circuit positions influence on the field asymmetry with the chosen tolerance value on the short circuits position ± 0.1 mm is negligible.

9 T-JUNCTION

The tuning of T-junctions was conducted according to the known technique in which the matching of terminal loads ($VSWR \leq 1.03$ at $f = 2998$ MHz) and inductive slots were used. Without a slot we had the VSWR value 2.03 and the phase value -52° , that corresponded to the normalized conductivity value $1+j0.7$. After insertion of the inductive slot with the conductivity value $-j0.7$ into the position $l = 0.078\lambda_b$ from the T-junction flange (that corresponds to the slot width $a' = 46.1$ mm and thickness $t = 2.4$ mm) we obtained $VSWR=1.1$ and $\varphi = 93^\circ$. By means of changing a' till it equals 47 mm and l by 0.5 mm (which corresponds to the distance between the T-junction central plane and the slot position $l = 111.4$ mm) we obtained $\rho \leq 1.04$.

MAFIA-based calculations carried out by S.V. Ivanov at DESY have given the following results : $VSWR=1.034$ at $l = 111.5$ mm, $a' = 47$ mm, $t = 2$ mm.

The non-resonant perturbation method [6] was used for measurements of electric field at the coupler symmetry plane. A dielectric lead oriented along the electric

field lines in the feeding rectangular guide was moved along the y-axis (see Fig.1). The values of $\sqrt{\Gamma}$ which are proportional to the electric field strength versus y are presented in Fig.20. They were measured for the input coupler.

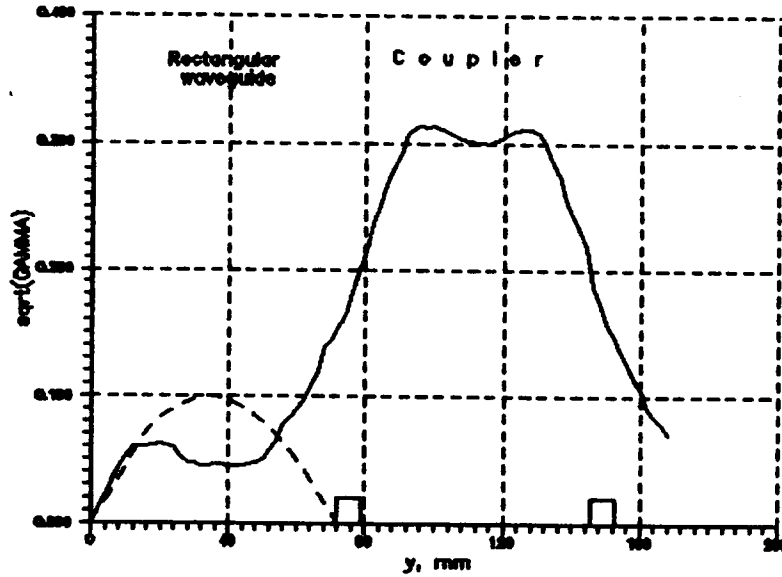


Fig.20 : Distribution of $\sqrt{\Gamma}$ depends on y-coordinate
 1) in the input coupler with rectangular waveguide;
 2) in the flat waveguide.

For calibration a perturbing bead was placed into uniform part of the feeding guide (dashed line in Fig.20). Calibrations were carried out on the basis of the expression for the H_{10} -mode electrical field in the rectangular waveguide [7].

$$E_y = 2\sqrt{\frac{P}{2ab}} \frac{\sqrt{Z_0}}{\sqrt{1 - \left(\frac{\lambda}{2a}\right)^2}} \quad (24)$$

If $P = 75 \text{ MW}$ and $a \times b = 34 \times 72 \text{ mm}^2$, $Z_0 = 377$ then $E = 8.2 \frac{\text{MV}}{\text{m}}$, which corresponds to $\sqrt{|\Gamma|_{\max}} = 0.1$.

10 REFERENCES

- [1] N.P. Sobenin, S.I. Ivanov, V.E. Kaljuzhny " The Investigation of Coupler for Linear Collider Acceleration section ", Proc of the Third European Particle Accelerator Conference, 1992, v. 2, pp 1226-1227.
- [2] H. Deruyter, H. Hoag, K. Ko, C.-k. Ng " Symmetrical Double Input Coupler Development ", SLAC-PUB-5887, August 1992.
- [3] N. Holtkamp, T. Weiland et al " Structure Work for an S-band Linear Collider ", Proc of XV International Conference on High Energy Accelerators, 1992, v. 2, pp 830-832.
- [4] V.E. Kalyuzhny, V.K. Vikulov " Investigation of Travelling Wave Accelerating Section High Frequency Characteristics on the Basis of Resonant Models ", Journal of Technical Physics, v. 52. No 11, 1982, pp. 2168-2176.
- [5] O.A. Valdner, N.P. Sobenin et al " Handbook of Disk Loaded Waveguide ", Moscow, Energoatomizdat, 300 pages, 1991.
- [6] N.P. Sobenin, B.V. Zverev " Electrodynamics Characteristics of Accelerating Cavities ", Moscow, Energoatomizdat, 220 pages, 1993.
- [7] O.S. Milovanov, N.P. Sobenin. " Microwave Technique ", Moscow, Atomizdat, 450 pages, 1980.